A one dimensional model of blood flow through a curvilinear artery

Fredrik Berntsson, Arpan Ghosh, Vladimir Kozlov and S. A. Nazarov

The self-archived postprint version of this journal article is available at Linköping University Institutional Repository (DiVA):
http://urn.kb.se/resolve?urn=urn:nbn:se:liu:diva-151627

N.B.: When citing this work, cite the original publication.
Berntsson, F., Ghosh, A., Kozlov, V., Nazarov, S. A., (2018), A one dimensional model of blood flow through a curvilinear artery, *Applied Mathematical Modelling*, 63, 633-643.
https://doi.org/10.1016/j.apm.2018.07.019

Original publication available at:
https://doi.org/10.1016/j.apm.2018.07.019

Copyright: Elsevier
http://www.elsevier.com/

Tweet

LINKÖPING UNIVERSITY

A ONE DIMENSIONAL MODEL OF BLOOD FLOW THROUGH A CURVILINEAR ARTERY

F. BERNTSSON, A. GHOSH*, V. A. KOZLOV, AND S. A. NAZAROV

Abstract. We present a one-dimensional model describing the blood flow through a moderately curved and elastic blood vessel. We use an existing two dimensional model of the vessel wall along with Navier-Stokes equations to model the flow through the channel while taking factors, namely, surrounding muscle tissue and presence of external forces other than gravity into account. Our model is obtained via a dimension reduction procedure based on the assumption of thinness of the vessel relative to its length. Results of numerical simulations are presented to highlight the influence of different factors on the blood flow.

1. Introduction

One of the most important systems in the human body is the circulatory system which performs a number of tasks like supplying nutrition throughout the body, regulation of body temperature and fighting diseases. It is also susceptible to various kinds of diseases. Simulating the system with a reasonable model can be of great help in managing problems arising in the system by aiding in early diagnosis. Substantial efforts have been made to model blood flow through blood vessels, see, for example, the monograph [8]. The complex arrangement of elastic tissues forming a blood vessel raises the difficulty in accurately modeling the interaction of blood flow with the vessel wall. The vessel walls have a laminate structure consisting of three layers of tissues (called adventitia, media and intima) having different composition and elastic properties, see [7].

In order to simulate blood flow efficiently, it is common practise to derive one-dimensional models. Some one-dimensional models are based on the conservation of fluid mass and momentum together with a linear stationary tube law resulting in, after an intrinsic linearization, a hyperbolic type equation with respect to pressure; or another longitudinal variable. Such models are described in detail in [10, 16, 23, 26, 27], where one can find more detailed analysis and references to miscellaneous variants of such models. Some other approaches use various shell models to coupled with Navier-Stokes equations to model the interaction of the elastic walls with the blood flow for a blood vessel having a cylindrical reference geometry by introducing some simplifying assumptions on the wall structure, see for example [24, 29]. Navier equations for the wall coupled with Navier-Stokes equations are also used in modeling the elastic walls, see [8, 25, 28]. However, the existing models, and even more elementary versions of the model presented in this article, such as [2, 13–15], only deal with the walls of straight sections of arteries despite the natural existence of their

S. A. Nazarov acknowledges the support from Russian Foundation of Basic Research, grant 18-01-00325.

curvilinear forms in the circulatory system. The curvilinearity of the vessels also arise as a result of movement of parts of the body. Hence, taking the curvilinearity of the vessels into account should result in more realistic simulations of blood flow.

The goal of this article is to derive a one-dimensional model describing the flow of blood through a curved blood vessel (with limited curvature) having an elastic wall and a varying radius for the cross-sections. Considering a variable radius in our model makes it particularly relevant to model diseases such as stenosis, see [18, 19]. To include the effects of the elastic wall on the blood flow, we consider a new two-dimensional model of elastic and layered vessel walls derived in [9] which includes the mechanical influence of the tissues surrounding the vessel along with an extra term in representing other external influences. Assuming that the width of the channel is small compared to the length of the vessel, we perform dimension reduction adapting the classical scheme of asymptotic analysis, cf. [4,21], in accordance with the curvilinear coordinate system used. We perform some numerical experiments on the resulting model in order to study the effects of the geometry of the vessel as well as to check the reasonableness of the model to an extent that is achievable for without realistic data.

1.1. **Formulation of the problem.** For the segment of a blood vessel considered here, we denote its hollow interior by Ω. We consider the vessel wall to be approximated by a two dimensional elastic surface described by a new model derived in [9]. We denote this two dimensional surface forming the boundary of the lumen leaving two open ends, by Γ. As in [9], we assume that a central curve is given for this vessel. The vessel is a deformed cylindrical hollow pipe around this given central curve. We assume the central curve to be sufficiently smooth. We also assume a circular cross-section of the vessel all along the central curve. This assumption is based on an optimal property of the cross-section of a vessel presented in [15]. And finally, we assume that the radius of curvature of the central curve is big compared to the radius of any cross-section of the vessel.

It should be noted at this point that the ambient three dimensional space is taken to have a canonical Cartesian coordinate system. We shall express any new coordinate system with the help of these coordinates.

Next, we introduce notations for the physical quantities involved in the modelling. The considered time interval is $[0, T]$, where T is the period of the cardiac cycle. The velocity field inside the blood channel within the vessel which describes the velocity of blood particles at a certain location of the lumen at a given time, is represented by $\mathbf{v} : \Omega \times [0, T] \to \mathbb{R}^3$. The displacement field in the vessel wall that measures the position of a point in the wall at a given time compared to its position in the original stress free state, is denoted by $\mathbf{u} : \Gamma \times [0, T] \to \mathbb{R}^3$. Let $p : \Omega \times [0, T] \to \mathbb{R}$ be the kinematic pressure of the fluid, which is directly proportional to the pressure within the fluid in the vessel as we take the density of the blood, ρ_b, to be constant in this case. For our model, $\mathbf{v}$, $\mathbf{u}$ and p are the unknowns in the equations.

The flow of blood through the vessel is assumed to be incompressible while satisfying the Navier-Stokes equation. The typical scales of the blood velocity $\mathbf{v}$ make sure that the effects from the non-linear term in the Navier-Stokes equation are insignificant and plays

no part in the asymptotic analysis. Hence we discard this term from the start. These considerations provide the following equations for our model:

$$\partial_t \mathbf{v} - \nu \Delta \mathbf{v} + \nabla p = \mathbf{g} \quad \text{in} \quad \Omega \times (0,T), \tag{1.1}$$

$$\nabla \cdot \mathbf{v} = 0 \quad \text{in} \quad \Omega \times (0,T), \tag{1.2}$$

where $\nu > 0$ is the dynamic viscosity of blood and $\mathbf{g}$ is the acceleration due to gravity and t is the time parameter.

We obtain further relations between the unknowns $\mathbf{v}$, $\mathbf{u}$ and p through appropriate boundary conditions on Γ. A no-slip assumption gives us

$$\mathbf{v} = \partial_t \mathbf{u} \quad \text{on} \quad \Gamma \times (0,T). \tag{1.3}$$

The last boundary condition is provided by the two dimensional model of the elastic vessel wall that was recently derived in [9]. This model is based on the assumption that the vessel walls are linearly elastic. Even though the vessel walls are non-linearly elastic in reality, this assumption is still reasonable and commonly accepted as it enables numerically solving the problem efficiently while still retaining the main mechanical properties of the vessel wall, see [6]. Moreover, the problem can be linearized when the deformations are small around some equilibrium points in the cycle of loading and unloading, see [25].

Assuming a coordinate system defined by the basis vectors $\{\mathbf{y}_1, \mathbf{y}_2, \mathbf{y}_3\}$ that shall be defined in a later section, the model for the vessel wall is given as

$$ME^*QEU + \bar{\rho}\partial_t^2 U + h^{-1}R^{-1}aKU = h^{-1}R^{-1}a(F_{ext} - \rho_b F) \quad \text{on} \quad \Gamma \times (0,T). \tag{1.4}$$

Here, h is the mean thickness of the vessel wall relative to some chosen reference radius R of the vessel. Thus hR is the true mean thickness of the vessel wall. Note that this factor arises here due to the lack of normalization of the forces as opposed to what is originally done in [9]. U, F_{ext} and F are the coordinate columns corresponding to the displacement vector $\mathbf{u}$, the resulting external force $\mathbf{f}$ acting on the vessel wall and the hydrodynamic force $\mathbf{F}$ exerted by the fluid on the wall respectively, expressed in the covariant basis corresponding to the basis mentioned above. The matrix M represents the metric tensor for the coordinate system. The function $a > 0$ contains the information on the laminar structure of the vessel wall so that multiplying it by the distance from the inner surface of the wall gives a constant for all the points in a single layer. The matrix K represents the tensor corresponding to the elastic response of the surrounding muscle tissues. We have E as a differential operator with E^* being its conjugate. Lastly, Q is a matrix representing the effective stiffness of the vessel wall.

In terms of the pressure and the velocity of the fluid, the hydrodynamic force is given as

$$\mathbf{F} = -p\mathbf{n} + \nu(\nabla \mathbf{v} + \nabla \mathbf{v}^T)\mathbf{n}. \tag{1.5}$$

2. Geometric setup

2.1. **Setting up a curvilinear coordinate system.** As we are modelling curved vessels, we first and foremost need to construct a suitable curvilinear coordinate system that simplifies the resulting expressions and computations to some extent. We start with the given centre curve and let it be represented by $\mathbf{c} \in \mathcal{C}^2([0,L], \mathbb{R}^3)$. Here, L is the total length

of the vessel. We assume $\mathbf{c}$ to be arc-length parameterised with s being the arc-length parameter. For simplicity, we assume $\mathbf{c}(0) = (0,0,0)^T$ and $\mathbf{c}'(0) = (0,0,1)^T$. Note that we denote the derivative of any function f that depends only on one parameter by f'.

Next, we build a right handed coordinate frame at each point $\mathbf{c}(s)$. The first obvious choice is to take one of the coordinate directions to be $\mathbf{c}'(s)$ (which is a unit vector, $\mathbf{c}$ being arc-length parameterised) and then the other two unit vectors to be perpendicular to it. We choose the rotation minimizing frame (see [3, 12]) consisting of the triplet $\{\mathbf{e}_1(\theta,s), \mathbf{e}_2(\theta,s), \mathbf{c}'(s)\}$ where $\mathbf{e}_i$ are obtained by solving

$$\partial_s \mathbf{e}_i(\theta,s) = -(\mathbf{c}''(s)\cdot \mathbf{e}_i(\theta,s))\mathbf{c}'(s)$$

with the initial conditions

$$\mathbf{e}_1(\theta,0) = (\cos\theta, \sin\theta, 0)^T \text{ and } \mathbf{e}_2(\theta,0) = (-\sin\theta, \cos\theta, 0)^T.$$

Additionally, they also satisfy

$$\partial_\theta \mathbf{e}_1(\theta,s) = \mathbf{e}_2(\theta,s) \text{ and } \partial_\theta \mathbf{e}_2(\theta,s) = -\mathbf{e}_1(\theta,s).$$

The parameter $\theta \in [0, 2\pi)$ signifies the direction from a point on $\mathbf{c}$ along the plane perpendicular to $\mathbf{c}'$ at that point with respect to some reference direction.

We need one more parameter to complete the new coordinate system for the three dimensional space surrounding the centre curve. Let R be a chosen reference radius for the vessel and $\alpha > 0$ be a suitable scaling depending on s. Thus, for any s, $R\alpha(s)$ gives the true distance of the vessel wall from the centre line $\mathbf{c}$. Let r denote the remaining parameter such that $r\alpha$ is the shortest distance of a point in the vessel from the centre curve $\mathbf{c}$. Clearly, $0 \le r \le R$.

Thus, the parameters r, θ and s give us our required coordinate system for the curvilinear vessel. Note that in the absence of curvature in the central curve and a constant radius of the vessel, this coordinate system coincides with the usual cylindrical coordinate system. The relation between the Cartesian and the new curvilinear coordinate systems is

$$\mathbf{x}(r,\theta,s) = \mathbf{c}(s) + r\alpha(s)\mathbf{e}_1(\theta,s), \quad 0 \le r \le R. \tag{2.1}$$

2.2. **Basis vectors and differential operators.** We go on to define the basis vectors corresponding to the new coordinates (r,θ,s). Using these basis vectors we can express the vectors, tensors as well as the differential operators appearing in the model equations. See Appendix D of [17] for a detailed presentation of tensor algebra in curvilinear coordinates.

Henceforth, we use the compact notations $\partial_1 = \partial/\partial r$, $\partial_2 = \partial/\partial\theta$ and $\partial_3 = \partial/\partial s$. Furthermore, we adopt Einstein's summation convention, according to which a sum over the the index set $\{1,2,3\}$ is implied for indices that occur concurrently at top and bottom in a term.

We define contravariant basis vectors representing the directions of increment of the new parameters r, θ and s respectively, for vectors defined inside the vessel. Let $\mathbf{x}_i = \partial_i \mathbf{x}$ for $i = 1,2,3$ and some $\mathbf{x} \in \Gamma$. Using (2.1) and writing $\beta := 1 - r\alpha\mathbf{c}''\cdot\mathbf{e}_1$, we have

$$\mathbf{x}_1 = \alpha\mathbf{e}_1, \quad \mathbf{x}_2 = r\alpha\mathbf{e}_2 \quad \text{and} \quad \mathbf{x}_3 = \beta\mathbf{c}' + r\alpha'\mathbf{e}_1. \tag{2.2}$$

This leads to the matrix representation of the metric tensor as $g_{ij} = \mathbf{x}_i \cdot \mathbf{x}_j$ for $i, j = 1, 2, 3$. Let g denote the matrix $[g_{ij}]$. Then, (2.2) leads to

$$g = \begin{bmatrix} \alpha^2 & 0 & r\alpha\alpha' \\ 0 & r^2\alpha^2 & 0 \\ r\alpha\alpha' & 0 & \beta^2 + r^2\alpha'^2 \end{bmatrix}. \tag{2.3}$$

As we average certain quantities over a cross-section for a fixed but arbitrary s as part of the dimension reduction procedure, it is worthwhile to mention here that the infinitesimal surface element for fixed s is given as

$$\mathrm{d}S = \sqrt{g_{11}g_{22} - g_{12}^2}\ \mathrm{d}r\mathrm{d}\theta = r\alpha^2\,\mathrm{d}r\mathrm{d}\theta. \tag{2.4}$$

The matrix representing the inverse metric tensor, $g^{-1} := [g^{ij}]$, then has the form

$$g^{-1} = \begin{bmatrix} \alpha^{-2}(1 + \beta^{-2}r^2\alpha'^2) & 0 & -\beta^{-2}\alpha^{-1}r\alpha' \\ 0 & r^{-2}\alpha^{-2} & 0 \\ -\beta^{-2}\alpha^{-1}r\alpha' & 0 & \beta^{-2} \end{bmatrix}. \tag{2.5}$$

The corresponding covariant basis vectors for the same space (see appendix D of [17]) are given as $\mathbf{x}^i = g^{ij}\mathbf{x}_j$. Clearly, this results in $\mathbf{x}^i \cdot \mathbf{x}_j = \delta^i_j$ with δ^i_j being the Kronecker delta. This also means that the vector $\mathbf{x}^1$ always aligns with the normal to a surface having a constant r, which makes it reasonable to express the vectors in our model in this basis. For our case, we have

$$\mathbf{x}^1 = \alpha^{-1}(\mathbf{e}_1 - \beta^{-1}r\alpha'\mathbf{c}'), \quad \mathbf{x}^2 = r^{-1}\alpha^{-1}\mathbf{e}_2 \quad \text{and} \quad \mathbf{x}^3 = \beta^{-1}\mathbf{c}'. \tag{2.6}$$

We can now express the gradient operator in terms of partial derivatives with respect to the new coordinates as

$$\nabla = \mathbf{x}^i\partial_i = \alpha^{-1}(\mathbf{e}_1 - \beta^{-1}r\alpha'\mathbf{c}')\partial_1 + r^{-1}\alpha^{-1}\mathbf{e}_2\partial_2 + \beta^{-1}\mathbf{c}'\partial_3. \tag{2.7}$$

We then have the Laplacian as

$$\begin{aligned} \Delta = \nabla \cdot \nabla &= \mathbf{x}^i\partial_i \cdot \mathbf{x}^j\partial_j \\ &= \alpha^{-2}(1 + \beta^{-2}r^2\alpha'^2)\partial_1^2 + r^{-2}\alpha^{-2}\partial_2^2 + \beta^{-2}\partial_3^2 - 2\beta^{-2}\alpha^{-1}r\alpha'\partial_1\partial_3 \\ &\quad + \alpha^{-1}(r^{-1}\alpha^{-1} - \beta^{-1}[(1 - \beta^{-2}r^2\alpha'^2)\mathbf{c}'' \cdot \mathbf{e}_1 + r\partial_3(\beta^{-1}\alpha')] + 2\beta^{-2}\alpha^{-1}r\alpha'^2)\partial_1 \\ &\quad - (\beta r\alpha)^{-1}\mathbf{c}'' \cdot \mathbf{e}_2\partial_2 - \beta^{-3}(\partial_3\beta - r\alpha'\mathbf{c}'' \cdot \mathbf{e}_1)\partial_3. \end{aligned} \tag{2.8}$$

At this point, we note that in our case, $\mathbf{x}_2 = r\alpha(s)\mathbf{e}_2(\theta, s)$ where $r \leq R$. In order to obtain the required model, we make use of the fact that the reference radius R of the vessel is small compared to the length of the vessel in consideration. This makes both the bases inconvenient to use for the asymptotic procedure as $\mathbf{x}_2$ is vanishingly small while while $\mathbf{x}^2$ is exceedingly big. With this in mind, we introduce the rescaled basis vectors

$$\bar{\mathbf{x}}^1 = \mathbf{x}^1, \quad \bar{\mathbf{x}}^2 = r\mathbf{x}^2 = \alpha^{-1}\mathbf{e}_2 \quad \text{and} \quad \bar{\mathbf{x}}^3 = \mathbf{x}^3.$$

3. Modelling of the flow

We shall derive the one dimensional model in this section. We adapt the procedure laid out in [13, 14] to our case and perform dimension reduction on the model equations (1.1), (1.2), (1.3) and (1.4) by taking asymptotic expansions of the unknowns with respect to a small parameter of choice.

3.1. **Asymptotic ansats.** Noting that the radius of the vessel is small compared to the length considered here, that is to say $R << L$, we introduce the fast variable η such that $r = \delta\eta$ with $\delta = R/L$. We introduce another time parameter $\tau = \delta^2 t$ as well, cf. [13].

The model equations induce the following expansions for the displacement vector field in the vessel wall, the velocity field in the fluid channel and the pressure in the fluid:

$$\mathbf{u} = \delta\mathbf{u}_0 + \delta^2\mathbf{u}_1 + \dots, \tag{3.1}$$

$$\mathbf{v} = \delta^2\mathbf{v}_0 + \delta^3\mathbf{v}_1 + \dots, \tag{3.2}$$

$$p = \mathbf{x}\cdot\mathbf{g} + p_0 + \delta p_1 + \dots \quad . \tag{3.3}$$

Here, the vectors $\mathbf{u}_i$ and $\mathbf{v}_j$ have coordinates $(u_{i1}, u_{i2}, u_{i3})^T$ and $(v_{i1}, v_{i2}, v_{i3})^T$ respectively in the basis $\{\bar{\mathbf{x}}^1, \bar{\mathbf{x}}^2, \bar{\mathbf{x}}^3\}$.

Introduction of the new variables and the assumption on the radius of curvature of $\mathbf{c}$, that is, $|\mathbf{c}''| << R^{-1}$, give us $\beta = 1 + O(\delta) \Rightarrow \beta^{-1} = 1 + O(\delta)$. Using this, we can express the gradient and the Laplacian operators in terms of η and δ. From (2.7) and (2.8), we have

$$\nabla = \delta^{-1}(\bar{\mathbf{x}}^1\partial_\eta + \eta^{-1}\bar{\mathbf{x}}^2\partial_2) + \bar{\mathbf{x}}^3\partial_3 \tag{3.4}$$

and

$$\Delta = \delta^{-2}\alpha^{-2}(\partial_\eta^2 + \eta^{-1}\partial_\eta + \eta^{-2}\partial_2^2) - \delta^{-1}\alpha^{-1}(\mathbf{c}''\cdot\mathbf{e}_1\partial_\eta + \eta^{-1}\mathbf{c}''\cdot\mathbf{e}_2\partial_2) + \dots \quad . \tag{3.5}$$

3.2. **The one dimensional model.** We use the expansions stated in the previous subsection in the equations (1.1), (1.2) and (1.3) and compare the coefficients of the various orders of δ.

Comparison of the terms of order δ^{-1} in (1.1) results in

$$\partial_\eta p_0 = \eta^{-1}\partial_2 p_0 = 0.$$

This implies the solution $p_0(\eta, \theta, s; \tau) = p_0(s; \tau)$.

Matching the coeficients of δ^0 in (1.1) and those of δ in (1.2), we get the following system of equations:

$$-\nu\alpha^{-2}(\partial_\eta^2 v_{01} + \eta^{-1}\partial_\eta v_{01} + \eta^{-2}\partial_2^2 v_{01} - 2\eta^{-2}\partial_2 v_{02} - \eta^{-2}v_{01}) + \partial_\eta p_1 = 0, \tag{3.6}$$

$$-\nu\alpha^{-2}(\partial_\eta^2 v_{02} + \eta^{-1}\partial_\eta v_{02} + \eta^{-2}\partial_2^2 v_{02} + 2\eta^{-2}\partial_2 v_{01} - \eta^{-2}v_{02}) + \eta^{-1}\partial_2 p_1 = 0, \tag{3.7}$$

$$-\nu\alpha^{-2}(\partial_\eta^2 v_{03} + \eta^{-1}\partial_\eta v_{03} + \eta^{-2}\partial_2^2 v_{03}) + \partial_3 p_0 = 0, \tag{3.8}$$

$$\alpha^{-2}(\partial_\eta v_{01} + \eta^{-1}v_{01} + \eta^{-1}\partial_2 v_{02}) = 0. \tag{3.9}$$

The corresponding boundary condition from (1.3) is

$$\mathbf{v}_0 = \mathbf{0} \quad \Leftrightarrow \quad v_{01} = v_{02} = v_{03} = 0.$$

As a result of the boundary condition above, the solution to the Stokes equations given in (3.6), (3.7) and (3.9) is

$$v_{01} = v_{02} = 0 \text{ and } p_1 = p_1(s;\tau).$$

On the other hand, the solution to the Drichlet problem for the Poisson equation (3.8) is

$$v_{03}(\eta,\theta,s;\tau) = \frac{\eta^2 - L^2}{4\nu}\alpha(s)^2\partial_3 p_0(s;\tau).$$

With the help of (2.4), we average over the inflated circular cross-section to obtain

$$\tilde{v}_{01} = \tilde{v}_{02} = 0 \quad \text{and} \quad \tilde{v}_{03}(s;\tau) = -\frac{L^2}{8\nu}\alpha(s)^2\partial_3 p_0(s;\tau) \tag{3.10}$$

where we have used the notation $\tilde{v}_{0i} := \dfrac{1}{\pi L^2}\displaystyle\int_0^{2\pi}\int_0^L v_{0i}\eta \mathrm{d}\eta\mathrm{d}\theta$.

Now comparing the terms of order δ^2 in the condition (1.2), we have

$$\alpha^{-2}(\partial_\eta v_{11} + \eta^{-1}v_{11} + \eta^{-1}\partial_2 v_{12}) - \alpha^{-1}\eta\alpha'\partial_\eta v_{03} + \partial_3 v_{03} = 0.$$

Integrating over the inflated circular cross section of the vessel at s,

$$\int_0^{2\pi}\int_0^L (\partial_\eta v_{11} + \eta^{-1}v_{11} + \eta^{-1}\partial_2 v_{12})\eta\mathrm{d}\eta\mathrm{d}\theta = \int_0^{2\pi}\int_0^L \left(\eta\alpha'\alpha\partial_\eta v_{03} - \alpha^2\partial_3 v_{03}\right)\eta\mathrm{d}\eta\mathrm{d}\theta$$

$$\Rightarrow \quad \int_0^{2\pi} v_{11}(R,\theta,s;\tau)L\mathrm{d}\theta = \int_0^{2\pi}\partial_\tau u_{01}(\theta,s;\tau)L\mathrm{d}\theta = \frac{\pi L^4}{8\nu}\partial_3(\alpha(s)^4\partial_3 p_0(s;\tau)).$$

Here we have used the divergence theorem and the boundary condition for v_{11}. Introducing the notation $\tilde{u}_{0i} = \dfrac{1}{2\pi}\displaystyle\int_0^{2\pi} u_{0i}(\theta,s;\tau)\mathrm{d}\theta$ for the average displacement of the wall at a given cross-section, we obtain

$$\partial_\tau \tilde{u}_{01}(s;\tau) = \frac{L^3}{16\nu}\partial_3(\alpha(s)^4\partial_3 p_0(s;\tau)). \tag{3.11}$$

Next, we consider the two dimensional model for the vessel wall derived in [9]. Let us first define a basis namely $\{\mathbf{y}^1,\mathbf{y}^2,\mathbf{y}^3\}$ on the two dimensional wall of the vessel in accordance to that in [9] by

$$\mathbf{y}^1 = \frac{a\alpha\beta}{\sqrt{\beta^2 + (\delta L\alpha')^2}}\bar{\mathbf{x}}^1, \quad \mathbf{y}^2 = \bar{\mathbf{x}}^2 \quad \text{and} \quad \mathbf{y}^3 = \bar{\mathbf{x}}^3 + \frac{\delta L\alpha\alpha'}{\beta^2 + (\delta L\alpha')^2}\bar{\mathbf{x}}^1.$$

Hence the transformation matrix T for the coordinates of vectors to change from the basis $\{\bar{\mathbf{x}}^1, \bar{\mathbf{x}}^2, \bar{\mathbf{x}}^3\}$ to the basis $\{\mathbf{y}^1, \mathbf{y}^2, \mathbf{y}^3\}$ is

$$T = \begin{bmatrix} \frac{\sqrt{\beta^2+(\delta L\alpha')^2}}{a\alpha\beta} & 0 & -\frac{\delta L\alpha'}{a\beta\sqrt{\beta^2+(\delta L\alpha')^2}} \\ 0 & 1 & 0 \\ 0 & 0 & 1 \end{bmatrix} = \begin{bmatrix} \frac{1}{a\alpha} + O(\delta) & 0 & O(\delta) \\ 0 & 1 & 0 \\ 0 & 0 & 1 \end{bmatrix}.$$

The differential operator E in (1.4) is expressed as

$$E = \begin{bmatrix} \frac{a\alpha}{\delta L} + O(\delta^0) & \frac{1}{\delta L}\partial_2 & \alpha\alpha' + O(\delta) \\ -a\mathbf{c}'' \cdot \mathbf{e}_1 + O(\delta) & -\frac{\mathbf{c}''\cdot\mathbf{e}_2}{\alpha} + O(\delta) & \partial_3 + O(\delta) \\ -\sqrt{2}\delta La\alpha\alpha'\mathbf{c}'' \cdot \mathbf{e}_2 + O(\delta^2) & \frac{1}{\sqrt{2}}\partial_3 - \sqrt{2}\frac{\alpha'}{\alpha} & \frac{1}{\sqrt{2}\delta L}\partial_2 + O(\delta^0) \end{bmatrix}.$$

The conjugate operator E^* of E is given as

$$-E^* = \begin{bmatrix} -\frac{a\alpha}{\delta L}+O(\delta^0) & a\mathbf{c}''\cdot\mathbf{e}_1+O(\delta) & \sqrt{2}\delta La\alpha\alpha'\mathbf{c}''\cdot\mathbf{e}_2+O(\delta^2) \\ \frac{1}{\delta L}\partial_2+O(\delta) & \frac{\mathbf{c}''\cdot\mathbf{e}_2}{\alpha}+O(\delta) & \frac{1}{\sqrt{2}}(\partial_3-\frac{\nabla G}{a}\cdot\partial_3(\nabla G)+\frac{3\alpha'}{\alpha}+O(\delta)) \\ -\alpha\alpha'+O(\delta) & \partial_3-\frac{\nabla G}{a}\cdot\partial_3(\nabla G)+\frac{\alpha'}{\alpha}+O(\delta) & \frac{1}{\sqrt{2}\delta L}\partial_2+O(\delta^0) \end{bmatrix}.$$

We assume the matrix Q in terms of its components is $[q_{ij}]$. The matrices M and K in 1.4 are given as

$$M = \begin{bmatrix} 1/a^2 & 0 & 0 \\ 0 & \alpha^2 & 0 \\ 0 & 0 & 1+O(\delta) \end{bmatrix} \quad \text{and} \quad K = \begin{bmatrix} \kappa & 0 & 0 \\ 0 & 0 & 0 \\ 0 & 0 & 0 \end{bmatrix}.$$

Let us assume $\bar{F}_{ext} = (\bar{F}_{ext,1}, \bar{F}_{ext,2}, \bar{F}_{ext,3})^T$ to be the coordinates of the external force in the basis $\{\bar{\mathbf{x}}^1, \bar{\mathbf{x}}^2, \bar{\mathbf{x}}^3\}$. Then we have $F_{ext} = T\bar{F}_{ext}$. Now choosing only the leading order terms with respect to δ in (1.4), we have

$$\frac{1}{\delta L^2}\begin{bmatrix} \frac{1}{a^2} & 0 & 0 \\ 0 & \alpha^2 & 0 \\ 0 & 0 & 1 \end{bmatrix}\begin{bmatrix} a\alpha & 0 & 0 \\ -\partial_2 & 0 & 0 \\ 0 & 0 & -\frac{1}{\sqrt{2}}\partial_2 \end{bmatrix} Q \begin{bmatrix} a\alpha & \partial_2 & 0 \\ 0 & 0 & 0 \\ 0 & 0 & \frac{1}{\sqrt{2}}\partial_2 \end{bmatrix}\begin{bmatrix} \frac{u_{01}}{a\alpha} \\ \bar{u}_{02} \\ u_{03} \end{bmatrix}$$
$$+(\delta^5\bar{\rho}\partial_\tau^2 + \frac{a}{hL}K)\begin{bmatrix} \frac{u_{01}}{a\alpha} \\ \bar{u}_{02} \\ u_{03} \end{bmatrix} = \frac{a}{\delta hL}\begin{bmatrix} \frac{1}{a\alpha} & 0 & 0 \\ 0 & 1 & 0 \\ 0 & 0 & 1 \end{bmatrix}\left(\bar{F}_{ext} + \rho_b\begin{bmatrix} \mathbf{x}\cdot\mathbf{g} + p_0 \\ 0 \\ 0 \end{bmatrix}\right).$$

Rewriting component wise and assuming that G and α are independent of τ, we obtain

$$h\alpha^2(q_{11}u_{01} + q_{11}\partial_2 u_{02} + \frac{1}{\sqrt{2}}q_{13}\partial_2 u_{03}) + \delta^6 hL^2\rho_w\partial_\tau^2 u_{01} + \delta La\kappa u_{01}$$
$$= La(\bar{F}_{ext,1} + \rho_b(\mathbf{x}\cdot\mathbf{g} + p_0)),$$
$$-\alpha^2\partial_2(q_{11}u_{01} + q_{11}\partial_2 u_{02} + \frac{1}{\sqrt{2}}q_{13}\partial_2 u_{03}) + \delta^6 hL^2\rho_w\partial_\tau^2 u_{02} = La\bar{F}_{ext,2},$$
$$-\frac{1}{\sqrt{2}}\partial_2(q_{31}u_{01} + q_{31}\partial_2 u_{02} + \frac{1}{\sqrt{2}}q_{33}\partial_2 u_{03}) + \delta^6 hL^2\rho_w\partial_\tau^2 u_{03} = La\bar{F}_{ext,3}.$$

Averaging both sides over the circular cross section of the vessel wall, that is, by integrating over θ over 0 to 2π and diving by 2π while assuming Q to be independent of θ, we have the following equations to complete our one dimensional model:

$$\begin{aligned} h\alpha^2 q_{11}\tilde{u}_{01} + \delta La\kappa\tilde{u}_{01} + \delta^6 hL^2\rho_w\partial_\tau^2\tilde{u}_{01} &= La(\tilde{F}_{ext,1} + \rho_b(\mathbf{c}\cdot\mathbf{g} + p_0)), \\ \delta^6 hL^2\rho_w\partial_\tau^2\tilde{u}_{02} &= La\tilde{F}_{ext,2}, \\ \delta^6 hL^2\rho_w\partial_\tau^2\tilde{u}_{03} &= La\tilde{F}_{ext,3}. \end{aligned} \tag{3.12}$$

where, $\tilde{F}_{ext,i} = \dfrac{1}{2\pi}\displaystyle\int_0^{2\pi}\bar{F}_{ext,i}\mathrm{d}\theta$. In the case of an external force that is uniformly constant over space, we have that $\tilde{F}_{ext,i} = 0$ for $i = 1, 2$. Furthermore, for any contact force on the vessel wall, it is reasonable to assume that it acts primarily along the normal to the vessel wall and hence $\tilde{F}_{ext,i} = 0$ for $i = 1, 2$ are insignificant. Thus, in terms of the main quantities of interest, namely $\tilde{u}_{01}$ and p_0, the model can be summarized by the following two equations:

$$\begin{aligned} h\alpha^2 q_{11}\tilde{u}_{01} + \delta La\kappa\tilde{u}_{01} + \delta^6 hL^2\rho_w\partial_\tau^2\tilde{u}_{01} &= La(\tilde{F}_{ext,1} + \rho_b(\mathbf{c}\cdot\mathbf{g} + p_0)), \\ \partial_\tau\tilde{u}_{01} &= \frac{L^3}{16\nu}\partial_3(\alpha^4\partial_3 p_0). \end{aligned} \tag{3.13}$$

Recall that α is the relative change in radius of the cross section and the effects of the vessel wall and the surrounding tissue are represented by q_{11} and κ respectively.

4. Numerical implementation

In this section, we discuss our numerical implementation for solving the equations of our one dimensional model. Numerical simulations of blood flow in veins or arteries have been carried out by several authors, see e.g. [5, 20]. In contrast, our mathematical model can be solved with a simple and a very efficient numerical method.

The main quantities of interest are the radial displacement of the wall averaged over the circular boundary of any cross-section, $\bar{u}_r$ and the pressure averaged over a cross-section, $\bar{p}$ and the axial component of the flow velocity averaged over a cross-section, $\bar{v}_s$. For our case, neglecting the lower order terms, $\bar{v}_s \equiv \delta^2\tilde{v}_{03} = R^2L^{-2}\tilde{v}_{03}$, $\bar{u}_r = \alpha^{-1}\delta\tilde{u}_{01} = RL^{-1}\tilde{u}_{01}$ and $\bar{p} = \rho_b(\mathbf{c}\cdot\mathbf{g} + p_0)$. We choose to assume a uniform thickness of the wall layers for our numerical experiments, hence we can take $a \equiv 1$, see [9]. Expressed in the original time variable, these quantities satisfy

$$\tilde{F}_{ext,1}(s,t) + \bar{p}(s,t) = A(s)\alpha(s)\bar{u}_r(s,t) + B\alpha(s)\partial_t^2\bar{u}_r(s,t) \tag{4.1}$$

and

$$\alpha(s)\partial_t\bar{u}_r(s,t) = \frac{R^3}{16\mu}\partial_s(\alpha(s)^4(\partial_s\bar{p}(s,t) - \rho_b\mathbf{c}'\cdot\mathbf{g})) \tag{4.2}$$

for $0 < t < T$ and $0 < s < L$, where $\mu = \rho_b\nu$ is the dynamic viscosity of blood, $A(s) = hR^{-1}q_{11}\alpha(s)^2 + \kappa$ and $B = hR\rho_w$.

Since both $\bar{p}$ and $\bar{u}_r$ are periodic in t, with period T, it is natural to use a Fourier series representation,

$$\widehat{p}(s,\xi_k) = \frac{1}{\sqrt{T}}\int_0^T \bar{p}(s,t)\mathrm{e}^{-i\xi_k t}dt, \quad \xi_k = \frac{2\pi k}{T},\ k\in\mathbb{Z}.$$

Inserting (4.2) into (4.1) and denoting the corresponding Fourier coefficients of $\tilde{F}_{ext,1}$ by $\widehat{F}_{ext,1}$, we get the Fourier coefficients $\hat{p}(s,\xi_k)$ of the pressure $\bar{p}$ in the vessel,

$$\begin{aligned} 0 &= \partial_s(\alpha(s)^4(\partial_s\widehat{p}(s,0) - \sqrt{T}\rho_b\mathbf{c}'(s)\cdot\mathbf{g})),\\ \widehat{F}_{ext,1}(s,\xi_k) + \widehat{p}(s,\xi_k) &= \frac{iR^3}{16\mu\xi_k}\left(B\xi_k^2 - A(s)\right)\partial_s(\alpha(s)^4\partial_s\widehat{p}(s,\xi_k)) \end{aligned} \tag{4.3}$$

for $0<s<L$ and $k\in\mathbb{Z}\backslash\{0\}$.

Since the equation (4.3) is of second order, two boundary conditions are needed. In this article, we use

$$\partial_s\bar{p}(0,t) = \rho_b\mathbf{c}'(0)\cdot\mathbf{g} - \frac{8\mu}{R^2\alpha(0)^2}\bar{v}_s(0,t), \quad 0<t<T. \tag{4.4}$$

This means that we specify the mean flow velocity of the blood at $s=0$. At the end $s=L$, we use the Dirichlet condition

$$\bar{p}(L,t) = p_*(t), \quad 0\le\tau<T. \tag{4.5}$$

Having a Dirichlet condition at $s=L$ means that we have a well-posed problem for the zero frequency component $\hat{p}(s,0)$, and we can recover the mean pressure. On the other hand, the condition is not realistic for a blood vessel so the solutions become unrealistic as one approaches $s=L$. Therefore, we present the solutions only over a small part of the total length of the vessel so that being far away from the boundary limits the effects of the boundary condition (4.5).

In our implementation, we select an equidistant grid $\{s_i\}_{i=1}^N$, and $\{t_j\}_{j=0}^M$, such that $s_1=0$, $s_N=L$, $t_0=0$, and $t_M=T$. Note that since we have periodic boundary conditions in t the points t_0 and t_M are the same. The equation (4.3) is solved for each frequency ξ_k separately, using the standard finite difference approximation

$$\partial_s(\alpha^4(s_i)\partial_s\hat{p}(s_i,\xi_k)) \approx (\alpha^4_{i+1/2}(\hat{p}(s_{i+1},\xi_k)-\hat{p}(s_i,\xi_k)) - \alpha^4_{i-1/2}(\hat{p}(s_i,\xi_k)-\hat{p}(s_{i-1},\xi_k)))(\Delta s)^{-2}$$

where $\alpha^4_{i\pm1/2}$ denotes $\alpha(s)^4$ approximated at $s=s_i\pm\Delta s/2$. The Neumann condition (4.4) is implemented using a one-sided difference

$$\partial_s\hat{p}(s_1,\xi_k) \approx \left(-3\hat{p}(s_1,\xi_k) + 4\hat{p}(s_2,\xi_k) - \hat{p}(s_3,\xi_k)\right)(2\Delta s)^{-1}.$$

These approximations mean that the finite difference method is $\mathcal{O}(\Delta s^2)$ accurate. Note also that the resulting linear system of equations is *tri-diagonal* and can be solved very efficiently.

Remark 1. *The proper choice of boundary conditions is dependent on which quantities can be accurately measured at the respective boundaries $s=0$ and $s=L$. In the case where*

Physical Quantity	Symbol	Unit	Values
Density of blood	ρ_b	kg/m^3	1050
Density of wall	ρ_w	kg/m^3	1050
Dynamic viscosity of blood	$\mu(=\rho_b\nu)$	$kg/m\,s$	$5.1\cdot 10^{-3}$
Reference radius of vessel	R	m	$6.31\cdot 10^{-3}$
Relative thickness of wall	h		10.3%
Modulus of Elasticity of wall	q_{11}	Pa	$4.5\cdot 10^5$
Period in time	T	s	0.917
Acceleration due to gravity	$\lvert\mathbf{g}\rvert$	m/s^2	9.8

TABLE 1. The physical parameters that were used for our tests.

measurements of the mean flow velocity $\bar{v}_s$ at the boundaries are available, we differentiate the equation (4.3) with respect to s and obtain

$$0 = \partial_s(\alpha(s)^2\widehat{v}_s(s,0)),$$

$$\widehat{v}_s(s,\xi_k) = \frac{iR^2}{16\mu\xi_k}\partial_s\left[\alpha(s)^2\left(R\left(B\xi_k^2 - A(s)\right)\partial_s(\alpha(s)^2\widehat{v}_s(s,\xi_k)) - 2i\xi_k\widehat{F}_{ext,1}(s,\xi_k)\right)\right]$$

with $\widehat{v}_s(s,\xi_k)$ being the Fourier coefficients of $\bar{v}_s$. Thus we can solve a Dirichlet problem for the mean flow velocity $\bar{v}_s$ in the vessel.

Remark 2. *Once the pressure field $\bar{p}$ is computed, we obtain the radial displacement field $\bar{u}_r$ using equation (4.1), i.e.*

$$\widehat{u}_r(s,\xi_k) = (\alpha(s)(A(s) - B\xi_k^2))^{-1}(\widehat{F}_{ext,1}(s,\xi_k) + \widehat{p}(s,\xi_k)).$$

4.1. **Numerical Experiments.** In order to demonstrate that our model works well in practice and can produce realistic solutions, we present the results from some numerical simulations representing different geometries of the vessel. As a basis for our calculations, we use typical physical parameters that roughly correspond to the carotid artery for a healthy individual; see [22]. In addition to this, we assume that the muscle interaction term in (4.1), $\kappa = 10^6 Nm^{-3}$ in order to have a mild contribution on the solutions. Also, the flow velocity profile used in the boundary condition (4.4) were taken from [11], where an experimental velocity profile was presented. For both simulations, we pick an equidistant grid consisting of $N = 500$ grid points in the s-variable, and $M = 512$ points in the t-variable. This means that we attempt to recover frequency components in the range $\xi_k = 2\pi kT^{-1}$, for $-255 < k < 256$.

We consider the blood flow in the carotid artery under normal conditions as specified in Table 1. We use the above mentioned experimentally obtained mean velocity profile for the boundary condition 4.4. At the far end of the vessel, we use a constant pressure $\bar{p}(L,t) = p_*$, where $p_* = 80\,mmHg$, or $10.7\,kPa$. We also assumed external forces other than gravity to be absent. The equations (4.1) and (4.2) are linear and we can set any zero level for the pressure; in our calculations we let $R = 6.31\,mm$ to be the reference radius of the blood vessel when the pressure is at $11.5\,kPa$. Hence the wall displacement $\bar{u}_r$ can be

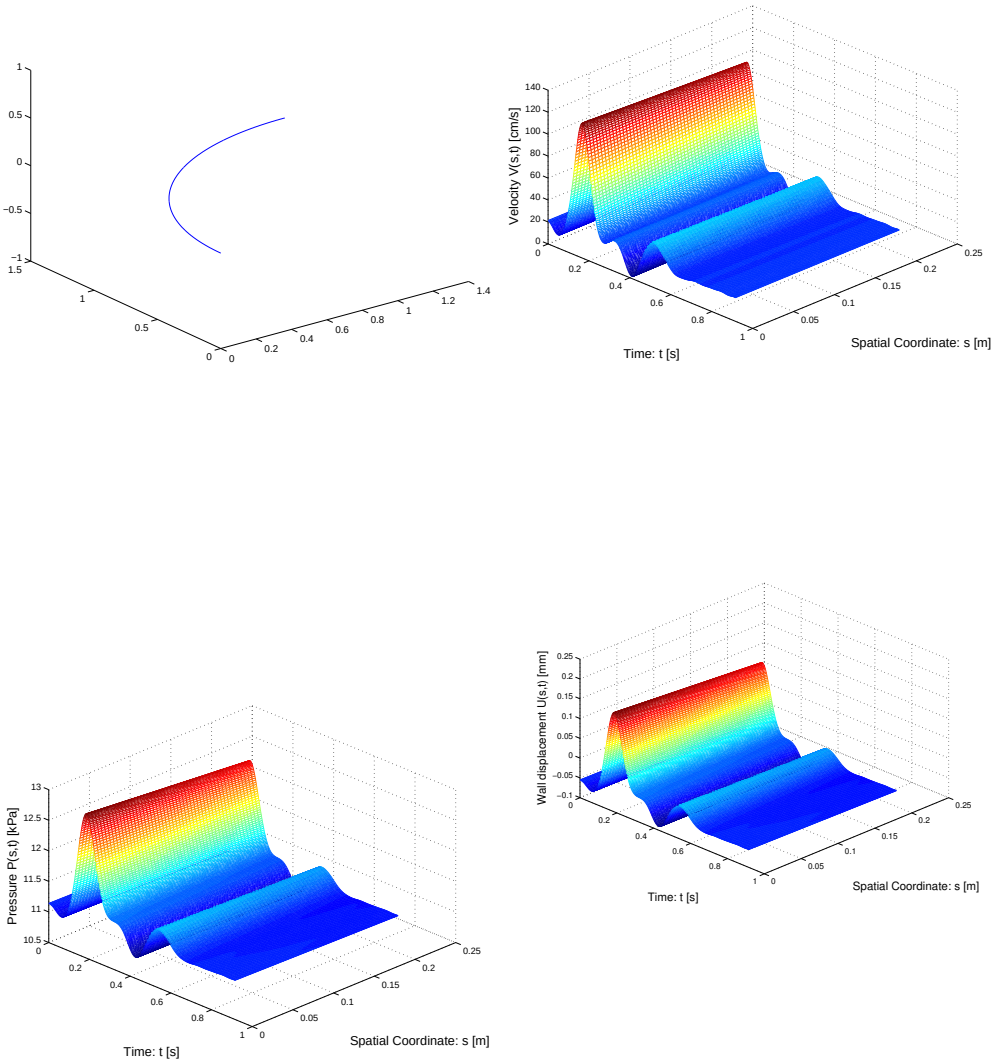

FIGURE 1. Results of Test 1: At the top left, the shape of the centre curve is depicted. The pictures at the top right, bottom left and bottom right show the calculated mean flow velocity profile $\bar{v}_s$, the mean pressure profile $\bar{p}$ and the mean radial displacement of the vessel wall $\bar{u}_r$ respectively along 10% of the centre curve over one time period.

both positive and negative. In the simulations, we only present the results in the interval $[0, L_0]$, for $L_0 = L/10$. In our cases, we consider centre curves of length L roughly $2m$ and thus the results presented are for approximately $20cm$. For the simulations, we take the last coordinate direction to be vertically upward and thus the first two as horizontal directions.

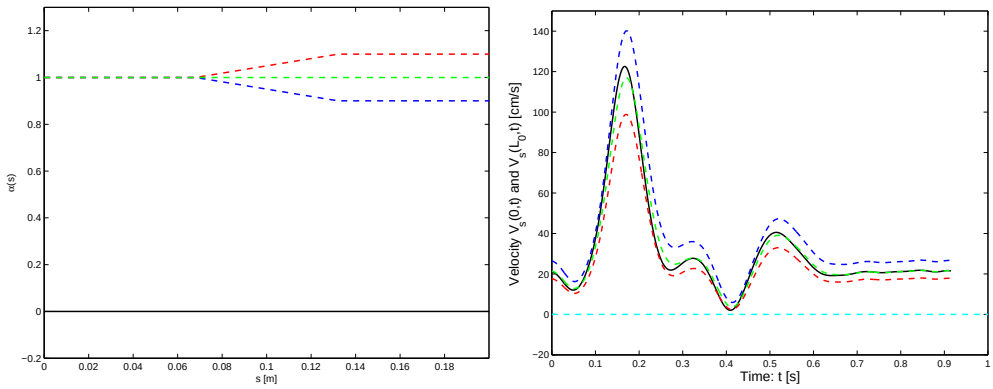

FIGURE 2. Results of Test 2: The picture on the left depicts three different cases for the function α. On the right, the flow velocities over one time period at about $20cm$ along the pipe are presented in colours corresponding to the α used. The velocity profile used at entry is plotted in black while the zero level is shown in cyan.

Test 1. *For the first case, we take the centre curve to be a spline joining the points* $(2 - 2\cos(k\pi/10), 2\sin(k\pi/10), 0)/\pi$ *for* $k = 1, 2, 3, 4, 5$ *which are taken from a circular arc. We assume a constant radius hence* $\alpha \equiv 1$*. The numerical results are presented in Figure 1. Note that the results closely resemble those in [2] as expected for this special case. This is due to the fact that the leading order terms of the pressure, the velocity of the flow as well as the displacement of the vessel wall are not affected by the shape of the centre curve unless it has a very high curvature (not considered here) or it curves along the direction of gravity.*

Test 2. *Once again we take the same curve as in the first test and study the effects of change of radius of the cross-section of the vessel. We perform the test with three different cases. One with a fixed radius, another with a narrowing vessel and lastly with widening vessel as shown in the plots for the function* α *in Figure 2. With the chosen shapes, we compare the flow velocities over time at about* $20cm$ *into the channel with the velocity profile used as the inflow condition. We see that under a fixed radius (plotted in green in Figure 2), the velocity remains largely the same with a slight drop in the peak velocity owing to the elastic effects of the vessel wall. In the case of a slightly shrinking vessel (plotted in blue), the velocity rises due to the conservation of mass of the fluid. The same reasoning explains the drop in velocity in the case of an expanding vessel (plotted in red).*

Test 3. *In this case, we consider a spline through the points* $(2-2\cos(k\pi/10), 2\sin(k\pi/10), k\pi/5)/(\sqrt{2}\pi)$ *for* $k = 1, 2, 3, 4, 5$ *which are taken from a helical arc. Thus we have a non trivial component of the flow direction along the direction of gravity. The resulting mean flow velocity, the pressure and the mean radial displacement of the vessel wall are depicted in Figure 3. We notice that while the pressure and the mean radial displacement fall off*

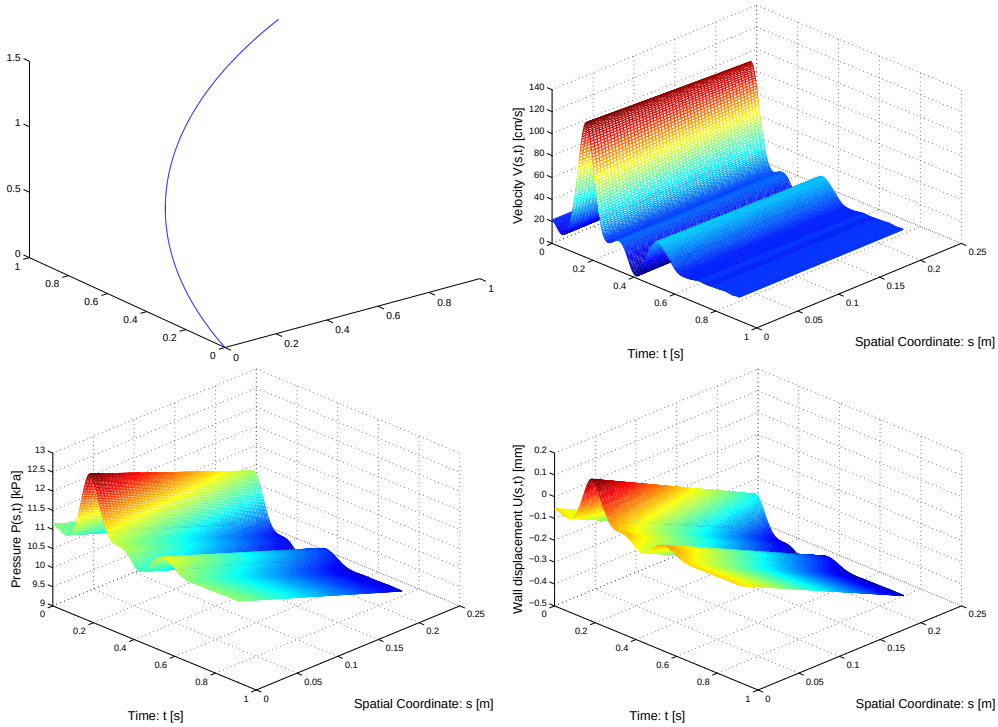

FIGURE 3. Results of test 3: The shape of the centre curve is shown in the picture at the top left. The pictures at the top right, bottom left and bottom right show the calculated mean flow velocity profile $\bar{v}_s$, the mean pressure profile $\bar{p}$ and the mean radial displacement of the vessel wall $\bar{u}_r$ respectively along 10% of the centre curve over one time period.

rapidly as one moves along the pipe, the mean flow velocity is approximately maintained which can be explained by the conservation of mass inside the channel.

Remark 3. *For the parameters used in our simulations, the coefficients of* $\bar{u}_r(s,t)$ *and* $\partial_t^2 \bar{u}_r(s,t)$ *in* (4.1) *for* $\alpha = 1$ *are respectively calculated to be*

$$A \equiv 8345500\, Nm^{-3} \quad \text{and} \quad B = 0.6824\, kgm^{-2}.$$

This means that under normal conditions in a healthy individual the inertia term $B\alpha(s)\partial_t^2 \bar{u}_r(s,t)$ *in (4.1) can be neglected leading to a simpler one-dimensional model:*

$$\tilde{F}_{ext,1} + \bar{p}(s,t) = A(s)\alpha(s)\bar{u}_r(s,t), \quad 0 \le t \le T,\ 0 < s < L.$$

5. Concluding Remarks

In this article, we have presented a simple one-dimensional model for blood flow in a curvilinear, elastic blood vessel with changing radius of the channel. The model is derived from the Navier-Stokes equations and a new model of the elastic walls of the vessel. Asymptotic analysis gives us the leading order terms constituting the model. Effects of

small curvature are only manifested in cases when the curvature has a non-zero component along the direction of gravity. We plan to extend the model to more general geometries in future. Effects of the surrounding muscle tissue and other external forces are also included in our model. Furthermore, we have tested our model by running simulations based on some typical physical characteristics of a normal carotid artery with some artificial boundary conditions and shown that the model provides reasonable solutions.

The simulations have been performed using a Dirichlet boundary condition at the outlet. This can result in somewhat unrealistic solutions. Hence we intend to investigate the model in future work using Robin boundary conditions based on loss coefficients (see for example [1]).

Furthermore, we intend to extend the model to the entire arterial tree. Since the basic model is one dimensional, and the numerical solution technique is efficient, we expect that the numerical calculations for the entire tree can be carried out in reasonable time.

References

[1] A. C. Benim, A. Nahavandi, A. Assmann, D. Schubert, P. Feindt, and S. H. Suh. Simulation of blood flow in human aorta with emphasis on outlet boundary conditions. *Appl. Math. Model.*, 35(7):3175–3188, 2011.

[2] Fredrik Berntsson, Matts Karlsson, Vladimir Kozlov, and Sergey A. Nazarov. A one-dimensional model of viscous blood flow in an elastic vessel. *Appl. Math. Comput.*, 274:125–132, 2016.

[3] R. L. Bishop. There is more than one way to frame a curve. *The American Mathematical Monthly*, 82:246–251, 1975.

[4] Philippe G. Ciarlet. *Mathematical elasticity. Vol. III*, volume 29 of *Studies in Mathematics and its Applications*. North-Holland Publishing Co., Amsterdam, 2000. Theory of shells.

[5] Francesco Fambri, Michael Dumbser, and Vincenzo Casulli. An efficient semi-implicit method for three-dimensional non-hydrostatic flows in compliant arterial vessels. *International Journal for Numerical Methods in Biomedical Engineering*, 30(11):1170–1198, 2014.

[6] Luca Formaggia, Alfio Quarteroni, and Allesandro Veneziani. *Cardiovascular Mathematics: Modeling and simulation of the circulatory system*, volume 1. Springer Science & Business Media, 2010.

[7] P. Fratzl, editor. *Collagen: Structure and Mechanics*. Springer US, 2008.

[8] Y. C. Fung. *Biomechanics: Circulation*. Springer-Verlag New York, 1997.

[9] A. Ghosh, V. A. Kozlov, S. A. Nazarov, and D. Rule. A two dimensional model of curvilinear blood vessels with layered elastic walls. *Submitted*, 2017.

[10] L. Grinberg, E. Cheever, T. Anor, J. R. Madsen, and G. E. Karniadakis. Modeling blood flow circulation in intracranial arterial networks: A comparative 3d/1d simulation study. *Annals of Biomedical Engineering*, 39(1):297–309, Jan 2011.

[11] D. W. Holdsworth, C. J. D. Norley, R. Frayne, D. A. Steinman, and B. K. Rutt. Characterization of common carotid artery blood-flow waveforms in normal human subjects. *Physiological Measurement*, 20(3):219, 1999.

[12] F. Klok. Two moving coordinate frames for sweeping along a 3d trajectory. *Computer Aided Geometric Design*, 3:217–229, 1986.

[13] V. A. Kozlov and S. A. Nazarov. Asymptotic models of blood flow in arteries and veins. *Zap. Nauchn. Sem. S.-Peterburg. Otdel. Mat. Inst. Steklov. (POMI)*, 409(Matematicheskie Voprosy Teorii Rasprostraneniya Voln. 42):80–106, 242, 2012.

[14] V. A. Kozlov and S. A. Nazarov. One-dimensional model of viscoelastic blood flow through a thin elastic vessel. *J. Math. Sci. (N.Y.)*, 207(2, Problems in mathematical analysis. No. 78 (Russian)):249–269, 2015.

[15] V. A. Kozlov and S. A. Nazarov. Asymptotic models of anisotropic heterogeneous elastic walls of blood vessels. *Journal of Mathematical Sciences*, 213(4):561–581, 2016.

[16] James Lighthill. *Mathematical biofluiddynamics*. Society for Industrial and Applied Mathematics, Philadelphia, Pa., 1975. Based on the lecture course delivered to the Mathematical Biofluiddynamics Research Conference of the National Science Foundation held from July 16–20, 1973, at Rensselaer Polytechnic Institute, Troy, New York, Regional Conference Series in Applied Mathematics, No. 17.

[17] A. I. Lurie. *Theory of Elasticity*. Springer, 2005.

[18] P. Kumar Mandal, S. Chakravarty, and A. Mandal. Numerical study of the unsteady flow of non-Newtonian fluid through differently shaped arterial stenoses. *Int. J. Comput. Math.*, 84(7):1059–1077, 2007.

[19] Kh. S. Mekheimer and M. A. El Kot. Mathematical modelling of unsteady flow of a Sisko fluid through an anisotropically tapered elastic arteries with time-variant overlapping stenosis. *Appl. Math. Model.*, 36(11):5393–5407, 2012.

[20] Lucas O. Müller, Carlos Parés, and Eleuterio F. Toro. Well-balanced high-order numerical schemes for one-dimensional blood flow in vessels with varying mechanical properties. *Journal of Computational Physics*, 242:53 – 85, 2013.

[21] S. A. Nazarov, A. Slutskij, and G. Sweers. Homogenization of a thin plate reinforced with periodic families of hard rods. *Mat. Sb.*, 202(8):41–80, 2011. (English transl.:Sb. Math. 2011. V. 202. N 8. P. 1127-1168).

[22] Niema M Pahlevan and Morteza Gharib. Aortic wave dynamics and its influence on left ventricular workload. *PLoS One*, 6(8):e23106, 2011.

[23] Timothy J. Pedley. Mathematical modelling of arterial fluid dynamics. *J. Engrg. Math.*, 47(3-4):419–444, 2003. Mathematical modelling of the cardiovascular system.

[24] A. Quarteroni and L. Formaggia. Mathematical modelling and numerical simulation of the cardiovascular system. In *Handbook of numerical analysis. Vol. XII*, Handb. Numer. Anal., XII, pages 3–127. North-Holland, Amsterdam, 2004.

[25] A. Quarteroni, M. Tuveri, and A. Veneziani. Computational vascular fluid dynamics: Problems, models and methods. *Comput. Vis. Sci.*, 2(4):163–197, March 2000.

[26] Philippe Reymond, Yvette Bohraus, Fabienne Perren, Francois Lazeyras, and Nikos Stergiopulos. Validation of a patient-specific one-dimensional model of the systemic arterial tree. *American Journal of Physiology - Heart and Circulatory Physiology*, 301(3):H1173–H1182, 2011.

[27] Charles A. Taylor and Mary T. Draney. Experimental and computational methods in cardiovascular fluid mechanics. In *Annual review of fluid mechanics. Vol. 36*, volume 36 of *Annu. Rev. Fluid Mech.*, pages 197–231. Annual Reviews, Palo Alto, CA, 2004.

[28] S. Čanić and A. Mikelić. Effective equations modeling the flow of a viscous incompressible fluid through a long elastic tube arising in the study of blood flow through small arteries. *SIAM J. Appl. Dyn. Syst.*, 2(3):431–463, 2003.

[29] S. Čanić, J. Tambača, G. Guidoboni, A. Mikelić, C. J. Hartley, and D. Rosenstrauch. Modeling viscoelastic behavior of arterial walls and their interaction with pulsatile blood flow. *SIAM J. Appl. Math.*, 67(1):164–193, 2006.

Mathematics and Applied Mathematics, MAI, Linköping University, SE 58183 Linköping, Sweden
Email address: fredrik.berntsson@liu.se

Mathematics and Applied Mathematics, MAI, Linköping University, SE 58183 Linköping, Sweden
Email address: arpan.ghosh@liu.se

Mathematics and Applied Mathematics, MAI, Linköping University, SE 58183 Linköping, Sweden
Email address: vladimir.kozlov@liu.se

St. Petersburg State University, 198504, Universitetsky pr., 28, Stary Peterhof, Russia; Institute of Problems of Mechanical Engineering RAS, V.O., Bolshoj pr., 61, St. Petersburg, 199178, Russia
Email address: srgnazarov@yahoo.co.uk